Indian Journal of Pure & Applied Physics
Vol. 58, July 2020, pp. 538-547

Finite element scheme for MHD forced convection flow near stagnation point and heat transfer by Newtonian heating, constant wall temperature and constant heat flux

Santosh Chaudhary[a]*, Mohan Kumar Choudhary[a] & Susheela Chaudhary[b]

[a]Department of Mathematics, Malaviya National Institute of Technology, Jaipur 302 017, India

[b]Department of Mathematics, Government Science College, Sikar 332 001, India

Received 17 January 2020; accepted 2 July 2020

Two dimensional, steady, forced convection magnetohydrodynamic flow of an incompressible, viscous electrically conducting fluid in a forward stagnation region of an infinite solid surface with Newtonian heating, constant wall temperature and constant heat flux has been investigated. Governing partial differential equations for the exploration have been formulated and converted to nonlinear ordinary differential equations by inserting convenient variables. An efficient finite element scheme along to Gauss elimination method has been introduced to find the numerical solutions of the resultant equations. Variation in velocity and temperature distributions against the pertinent parameters like magnetic parameter, Prandtl number and Eckert number have been displayed graphically while skin-friction coefficient and Nusselt number have been discussed quantitatively. A comparison of the computational results has been found in excellent agreement with open literature for limiting cases.

Keywords: MHD, forced convection, stagnation point, heat transfer, Newtonian heating, constant wall temperature, constant heat flux

1 Introduction

Free convection occurs due to the temperature difference of the fluid in its entire fluid domain while forced convection is the heat flow occurring due to externally applied forces. Forced convection is usually done to enlarge the heat transformation rate, which is brought about by various methods like enhancing the thermal conductivity, changing flow geometry and boundary conditions of the fluid. It plays a vital role in manufacturing and technological processes including mixing of one substance with another, heating and cooling of body parts by blood circulation, fluid radiator systems, cooling processes of foods, action of a propeller in a fluid and in aerodynamic heating. In all the above processes, it is imperative since the increment of the heat transfer rate from the body surface to encompassing liquid medium into reduce heat as much as possible. Although few improvements in the heat transfer properties can tend to considerable savings. In many electronic components like capacitors, solenoids, inductors and transistors, extrinsic fans are necessary to avoid component loss because natural convections have nearly low cooling ability. In the books of Nield and Bejan[1] and Shang[2], the relevant literature can be seen. Moreover, a lot of investigations have been studied on heat transfer flow over a plate along to forced convection by several researchers such as Seddeek[3], El-Amin[4], Duwairi[5] and Merkin and Pop[6]. Recently, Sasmal *et al.*[7], Chaudhary and Kumar[8], Satish and Venkatasubbaiah[9], Mohseni *et al.*[10], Atashafrooz *et al.*[11] and Sharma and Paul[12] have examined different aspects of forced convection and found computational solutions.

The flow of viscous fluid over a stagnation domain has a valuable bearing on various engineering and technical processes. So, the fluid flow nearby the stagnation domain has captured the attention of researchers for a long time period. Most of the time a line or stagnation point occurs inside the domain of flow but sometimes flow stagnates via a solid sheet. Stagnation region creates the highest pressure rate, the highest heat transfer and the highest mass decomposition rate. It should be noted that the solution of stagnation point flows are exist for a tiny domain in the stagnation point vicinity of a two or three dimensional frame but they produce a number of physical flows of technological and industrial

*Corresponding author (E-mail: d11.santosh@yahoo.com)

implication. This problem arises in a broad group of engineering procedures and industrial manufacturing particularly flow over the tips of rockets, blood flow problems, electronic devices cooling through fans, textile processes and paper industries, central collectors bared to wind currents, submarines, boundary layer with material conducting conveyers, plastic plates aerodynamic extrusion, oil ships and aircrafts. It is also noted that the velocity at stagnation point evolves along the increment in magnetic field for the stretching velocity is lesser the free stream velocity. Heimenz[13] initiated the boundary layer flow in the stagnation domain over an infinite surface. Later, Homann[14] extended the problem for axisymmetric case. Further various numerical and analytical explorations explaining different physical conditions of the fluid flow over a stagnation point are introduced by Eckert[15], Mahapatra and Gupta[16], Lok *et al.*[17] and Jat and Chaudhary[18]. Recently, Mahapatra and Nandy[19], Chaudhary and Choudhary[20], Mahapatra and Sidui[21], Dholey[22], and Fang and Wang[23] represented the stagnation point flow problem in different configurations.

In all of the above cited investigations, much applications has been gained to investigate the boundary layer flow towards heat transfer via either a constant heat flux at the surface or a constant wall temperature. After that, there is additional important case of boundary condition in which the surface heat transfer rate depends on the wall temperature linearly or nonlinearly. When the wall heat exchange rate is proportional to the temperature of local surface from the surrounding wall along to finite heat capacity, it is acknowledged as the conjugate convective flow or Newtonian heating. Although Newtonian heating is of utmost importance in the variety of mechanical instruments along with heat fins and heat exchangers, this heat transfer procedure is assumed to be negligible in the literature. Merkin[24] pioneered the analysis in this field and started to describe the term Newtonian heating in heat transfer problems. Later several authors like Pop *et al.*[25], Lesnic *et al.*[26], Merkin *et al.*[27], Hayat *et al.*[28], Kushwaha and Sahu[29], Chaudhary *et al.*[30] and Aghayari *et al.*[31] have studied Newtonian heating effect and convective heat transfer over various geometry of flow.

Analysis of motion of an electrically conducting fluid due to the influence of magnetic field is a topic of significance in heat transfer problems because of its numerous applications in different engineering and industrial problems like MHD marine propulsion, boundary layer domination in aerodynamics, ion propulsion, microelectronic devices, MHD power generators, nuclear reactors cooling, petroleum industries, crystal growth, MHD bearings and MHD pumps. In all the above processes, cooling rate and the appropriate final product characteristics may be contained via using the electrically conducting fluid in the existence of magnetic field. From last few decades the effect of magnetic field have presented extensively due to its frequent occurrence in many technological processes in geophysics, astrophysics and in the area of metallurgy like molten metal MHD stirring, magnetic-levitation casting, exotic lubricants and suspension solutions, solidification of liquid crystals, foodstuff processing and molten metal purification by non-metallic formations. Molten metal sprayed from a height on the substrate containing sulphides, oxides and silicates etc, as stagnation point flow, applied transverse magnetic field and electromagnetic force help to separate the non-metallic inclusions from the molten metal. Probably Andersson[32] examined the hydromagnetic flow of visco-elastic fluid past a stretching sheet. The investigation of MHD stagnation point flow towards a stretchable plate was discussed by Mahapatra and Gupta[33]. Following him, many researchers such as Abel and Mahesha[34], Chaudhary *et al.*[35], Chaudhary and Choudhary[36], Benos and Sarris[37], Chaudhary and Kanika[38] and Rao *et al.*[39] discussed different magnetohydrodynamic flow problems and presented numerical and analytical solutions considering several aspects of the problems.

Goal of the current analysis is to analyze a mathematical structure of the two dimensional, steady forced convection flow of an electrically conducting fluid nearby the forward stagnation point with the impacts of magnetic field and viscous dissipation. The same problem was also inspected by Salleh *et al.*[40] in the absence of magnetic field and the viscous dissipation near the plate which is very important in variety of technological processes. In the present paper, heat transfer is presented and compared in three different cases as Newtonian heating (NH), constant wall temperature (CWT) and constant heat flux (CHF) which is not available in literature yet. The obtained results represent productive information for application and can be used as a magnification of previous results.

2 Problem Formulation

Two-dimensional forced convection laminar stagnation point flow of a viscous incompressible

electrically conducting fluid at a solid plate is considered here. In this model rectangular coordinates are used and $x-$ and $y-$axes are taken corresponding to the infinite plate and perpendicular to it keeping origin at the stagnation point of the wall. A uniform magnetic field is applied with strength B_0, which is subjected to the fluid in the $y-$axis direction, as presented by Fig. 1. The magnetic Reynolds number is taken smaller than unity therefore induced magnetic field becomes very small in the comparison of the applied magnetic field, which can be decayed. Also, viscous dissipation near the sheet is also taken into the account. The external free stream flow velocity $u_e(x)=ax$ varies linearly along $x-$axis, where a is a positive constant and x is the coordinate measured forward the infinite surface. The temperature of ambient fluid is taken as a constant value T_∞. The wall is also subjected to a NH, CWT and CHF of the form $\left(\frac{\partial T}{\partial y}\right)_{y=0}=-h_s T$, $T=T_w$ and $\left(\frac{\partial T}{\partial y}\right)_{y=0}=-\frac{q_w}{\kappa}$ respectively, where T is the fluid temperature, $h_s=\sqrt{\frac{a}{\upsilon}}$ is a constant, υ is kinematic viscosity, T_w is the fluid temperature at the surface, q_w is the constant wall heat flux and κ is the thermal conductivity. Therefore, under the given considerations, the basic equations may be defined as follows (Bansal[41]):

$$\frac{\partial u}{\partial x}+\frac{\partial v}{\partial y}=0 \qquad \ldots (1)$$

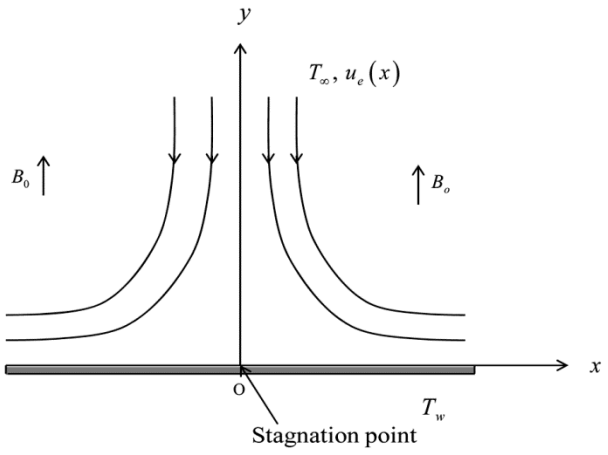

Fig. 1 — Flow configuration.

$$u\frac{\partial u}{\partial x}+v\frac{\partial u}{\partial y}=u_e\frac{du_e}{dx}+\upsilon\frac{\partial^2 u}{\partial y^2}-\frac{\sigma_e {B_0}^2}{\rho}(u-u_e) \qquad \ldots (2)$$

$$u\frac{\partial T}{\partial x}+v\frac{\partial T}{\partial y}=\alpha\frac{\partial^2 T}{\partial y^2}+\frac{\mu}{\rho C_p}\left(\frac{\partial u}{\partial y}\right)^2+\frac{\sigma_e {B_0}^2}{\rho C_p}(u-u_e)^2 \ldots (3)$$

along with the boundary conditions in the case of NH, CWT and CHF

$$y=0 \;:\; u=0,\; v=0,\; \frac{\partial T}{\partial y}=-h_s T\,(NH),\; T=T_w(CWT),\; \frac{\partial T}{\partial y}=-\frac{q_w}{\kappa}(CHF)$$
$$y\to\infty:\; u\to u_e(x),\; T\to T\infty \qquad \ldots (4)$$

where u and v are the velocity factors in the $x-$ and $y-$ directions, respectively, σ_e is the electrical conductivity, ρ is the fluid density, α is the thermal diffusivity, μ is the coefficient of viscosity and C_p is the specific heat at constant pressure.

3 Similarity Analysis

The governing equations (1) to (3) along with the boundary conditions equation (4) can be represented in dimensionless form by presenting the following non-dimensional variables (Salleh *et al.*[40]):

$$\psi(x,y)=x\sqrt{a\upsilon}\,f(\eta) \qquad \ldots (5)$$

$$\eta=\sqrt{\frac{a}{\upsilon}}y \qquad \ldots (6)$$

$$\theta(\eta)=\frac{T-T_\infty}{T_\infty}\,(NH),\quad \theta(\eta)=\frac{T-T_\infty}{T_w-T_\infty}\,(CWT),\quad \theta(\eta)=\frac{T-T_\infty}{h_s\frac{q_w}{\kappa}}\,(CHF)$$
$$\ldots (7)$$

$$u=\frac{\partial\psi}{\partial y},\quad v=-\frac{\partial\psi}{\partial x} \qquad \ldots (8)$$

where $\psi(x,\,y)$ is the stream function, $f(\eta)$ is the dimensionless stream function, η is the similarity variable and $\theta(\eta)$ is the dimensionless temperature.

Utilizing equations (5) to (8), the continuity equation (1) is satisfied automatically, and the momentum and the energy equations (2) and (3) are converted as:

$$f'''+ff''-f'^2-M(f'-1)+1=0 \qquad \ldots (9)$$

$$\frac{1}{\Pr}\theta''+f\theta'+Ecf''^2+MEc(f'-1)^2=0 \qquad \ldots (10)$$

subjected to reduced boundary conditions:

$\eta = 0 \;:\; f = 0,\; f' = 0,\; \theta' = -(1+\theta)\;\; (NH),\;\; \theta = 1\;\; (CWT),\;\; \theta' = -1\;\; (CHF)$
$\eta \to \infty :\; f' \to 1,\; \theta \to 0$

… (11)

where prime stands for differentiation with respect to η, $M = \frac{\sigma_e B_0^{\,2}}{\rho a}$ is the magnetic parameter, $\Pr = \frac{\upsilon}{\alpha}$ is the Prandtl number and $Ec = \frac{u_e^{\,2}}{C_p T_\infty}$ (NH), $Ec = \frac{u_e^{\,2}}{C_p (T_w - T_\infty)}$ (CWT) and $Ec = \frac{u_e^{\,2}}{C_p h_s \frac{q_w}{\kappa}}$ (CHF) is the Eckert number.

4 Solution Procedure

To find the computational solution of the Eqs (9) and (10) subjected to the appropriate boundary conditions Eq. (11), Galerkin finite element method is applied in association with Gauss elimination scheme. Initially, introducing a new dependent variable h such that:

$$f' = h \qquad \ldots (12)$$

Equations (9) to (11) were converted into the following set of differential equations:

$$h'' + fh' - h^2 - M(h-1) + 1 = 0 \qquad \ldots (13)$$

$$\frac{1}{\Pr}\theta'' + f\theta' + Ech'^2 + MEc(h-1)^2 = 0 \qquad \ldots (14)$$

with the reduced boundary conditions:

$\eta = 0 \;:\; f = 0,\;\; h = 0,\;\; \theta' = -(1+\theta)\;\; (NH),\;\; \theta = 1\;\; (CWT),\;\; \theta' = -1\;\; (CHF)$
$\eta \to \infty :\; h \to 1,\;\; \theta \to 0$

… (15)

For the computational procedure, the free stream boundary conditions at $\eta \to \infty$ is shifted to a sufficiently large finite value at $\eta \to \infty = 6$ which is very approximate to earn the properties of free stream flow field asymptotically being values of considered physical parameters. Further, the whole space is separated into 1000 equal two-nodded linear elements. These are continuous and the linear Lagrange polynomial formula is imposed for every typical element.

The weak form of Eqs (12) to (14) for an individual element (η_e, η_{e+1}), is considered as:

$$\int_{\eta_e}^{\eta_{e+1}} w_1 (f' - h)\, d\eta = 0 \qquad \ldots (16)$$

$$\int_{\eta_e}^{\eta_{e+1}} w_2 \left[h'' + fh' - h^2 - M(h-1) + 1\right] d\eta = 0 \quad \ldots (17)$$

$$\int_{\eta_e}^{\eta_{e+1}} w_3 \left[\frac{1}{\Pr}\theta'' + f\theta' + Ech'^2 + MEc(h-1)^2\right] d\eta = 0 \quad \ldots (18)$$

where w_1, w_2 and w_3 are weight functions related to the functions f, h and θ respectively.

Introducing the shape function φ_i for an element (η_e, η_{e+1})

$$\varphi_1^{(e)} = \frac{\eta_{e+1} - \eta}{\eta_{e+1} - \eta_e}, \quad \varphi_2^{(e)} = \frac{\eta - \eta_e}{\eta_{e+1} - \eta_e}, \quad \eta_e \le \eta \le \eta_{e+1}$$

and the finite element approximations are assumed of the form $f = \sum_{j=1}^{2} f_j \varphi_j$, $h = \sum_{j=1}^{2} h_j \varphi_j$ and $\theta = \sum_{j=1}^{2} \theta_j \varphi_j$ with $w_1 = w_2 = w_3 = \varphi_i, (i = 1, 2)$.

Now the element equations for Eqs (16) to (18) are assembled over the entire space using the connected inter-element condition, which provides a big number of linear equations also named a global finite element model.

$$\begin{bmatrix} [K^{11}] & [K^{12}] & [K^{13}] \\ [K^{21}] & [K^{22}] & [K^{23}] \\ [K^{31}] & [K^{32}] & [K^{33}] \end{bmatrix} \begin{bmatrix} \{f\} \\ \{h\} \\ \{\theta\} \end{bmatrix} = \begin{bmatrix} \{b^1\} \\ \{b^2\} \\ \{b^3\} \end{bmatrix} \qquad \ldots (19)$$

where $[K^{mn}]$ and $[b^m] (m = 1,2 \;\; and \;\; n = 1,2)$ are define as:

$$K_{ij}^{11} = \int_{\eta_e}^{\eta_{e+1}} \varphi_i \frac{d\varphi_j}{d\eta} d\eta, \;\; K_{ij}^{12} = -\int_{\eta_e}^{\eta_{e+1}} \varphi_i \varphi_j d\eta, \;\; K_{ij}^{13} = 0,$$

$$K_{ij}^{21} = 0, \;\; K_{ij}^{22} = \int_{\eta_e}^{\eta_{e+1}} \left[-\frac{d\varphi_i}{d\eta}\frac{d\varphi_j}{d\eta} + \bar{f}\,\varphi_i \frac{d\varphi_j}{d\eta} - (\bar{h} + M)\varphi_i \varphi_j \right] d\eta, \;\; K_{ij}^{23} = 0,$$

$$K_{ij}^{31} = 0, \; K_{ij}^{32} = Ec \int_{\eta_e}^{\eta_{e+1}} \left[\overline{h}'\varphi_i \frac{d\varphi_j}{d\eta} + M(\bar{h} - 2)\varphi_i \varphi_j \right] d\eta,$$

$$K_{ij}^{33} = \int_{\eta_e}^{\eta_{e+1}} \left[-\frac{1}{\Pr}\frac{d\varphi_i}{d\eta}\frac{d\varphi_j}{d\eta} + \bar{f}\,\varphi_i \frac{d\varphi_j}{d\eta} \right] d\eta$$

$$b_i^1 = 0, \quad b_i^2 = -\left(\varphi_i \frac{dh}{d\eta}\right)_{\eta_e}^{\eta_{e+1}} - (M+1)\int_{\eta_e}^{\eta_{e+1}} \varphi_i \, d\eta, \;\; b_i^3 = -\frac{1}{\Pr}\left(\varphi_i \frac{d\theta}{d\eta}\right)_{\eta_e}^{\eta_{e+1}} - MEc \int_{\eta_e}^{\eta_{e+1}} \varphi_i \, d\eta$$

and also

$$\bar{f} = \sum_{i=1}^{2} \bar{f}_i \varphi_i, \;\; \bar{h} = \sum_{i=1}^{2} \bar{h}_i \varphi_i, \;\; \bar{h}' = \sum_{i=1}^{2} \overline{h}_i' \varphi_i, \;\; \bar{\theta} = \sum_{i=1}^{2} \bar{\theta}_i \varphi_i.$$

Here the complete area of expertise is split into 1000 linear sub-domains. So the whole domain has 1001 nodes and at each node, three unknown

functions f, h and θ are to be determined. Therefore the element equations for entire domain are assembled and a matrix of order 3003×3003 is obtained. The system of 2998 equations remains to be solved via an iterative method after imposing the boundary conditions. To solve the set of linear equations in the present study, Gauss elimination method is applied. The step size is assumed as $\Delta\eta = 0.006$ and the iterative procedure is stopped when the following condition is fulfilled

$$\sum_i \left|\Phi_i^{j+1} - \Phi_i^{j}\right| \le 10^{-7}$$

where Φ stands for either f, h or θ and j represents the iterative step.

5 Physical Quantities

The local skin friction coefficient C_f and the local Nusselt number Nu_x are the important physical quantities of practical interest in present study which are given as:

$$C_f = \frac{\mu\left(\frac{\partial u}{\partial y}\right)_{y=0}}{\frac{\rho u_e^{\,2}}{2}} \qquad \ldots (20)$$

$$Nu_x = -\frac{x\left(\frac{\partial T}{\partial y}\right)_{y=0}}{T_w - T_\infty} \qquad \ldots (21)$$

Using the similarity variables (5) to (8), the equations (20) and (21) can be signified as:

$$C_f = \frac{2}{\sqrt{\mathrm{Re}_x}} f''(0) \qquad \ldots (22)$$

$$\frac{Nu_x}{\sqrt{\mathrm{Re}_x}} = -\frac{1}{\theta(0)}\theta'(0)\ (NH),\quad \frac{Nu_x}{\sqrt{\mathrm{Re}_x}} = -\theta'(0)\ (CWT),\quad \frac{Nu_x}{\sqrt{\mathrm{Re}_x}} = \frac{1}{\theta(0)}\ (CHF) \qquad \ldots (23)$$

where $\mathrm{Re}_x = \dfrac{u_e x}{\upsilon}$ is the local Reynolds number.

6 Numerical Method Validation

The proposed computational method, applied in the previous section is validated here. Table 1 shows the comparison of the results for the impact of various values of the Prandtl number Pr on the rate of heat transfer $\theta'(0)$ in the absence of the magnetic parameter M and the Eckert number Ec for the case of CWT with the earlier published works. Further, the numerical values of the temperature profile $\theta(0)$ in the case of CHF are also compared for different values of the Prandtl number Pr with the literature of previous researchers in the limiting cases. From the table, it is evident that the present study data are in superlative agreement with those researchers. The efficiency and the reliability of the obtained values are also claimed by the table.

7 Numerical Results and Discussion

This part is committed to bring out the variations in the velocity $f'(\eta)$, the temperature $\theta(\eta)$, the surface shear stress $f''(0)$ and the surface heat flux $\theta'(0)$ due to some pertinent parameters like the magnetic parameter M, the Prandtl number Pr and the Eckert number Ec. Computational results of the velocity $f'(\eta)$ and the temperature $\theta(\eta)$ are demonstrated through graphs while the computational results of the surface shear stress $f''(0)$ and the heat transfer rate $\theta'(0)$ are shown in table.

Table 1 — Comparison of $\theta'(0)$ and $\theta(0)$ for various values of Pr where $M = Ec = 0.0$ and $f''(0) = 1.232588$.

Pr	$-\theta'(0)$ (CWT)			$\theta(0)$ (CHF)		
	Eckert[15]	Salleh et al.[40]	Present Results	Lok et al.[17]	Salleh et al.[40]	Present Results
0.1		0.2195	0.2379586	4.5557	4.5557	4.202411
0.2		0.2964	0.3003920	3.3743	3.3742	3.328983
0.4		0.3958	0.3959727	2.5267	2.5267	2.525427
0.6		0.4663	0.4663406	2.1444	2.1444	2.144356
0.7	0.496	0.4959	0.4958680	2.0166	2.0166	2.016665
0.8	0.523	0.5228	0.5227418	1.9130	1.9130	1.912991
1.0	0.570	0.5705	0.5704650	1.7529	1.7529	1.752955
5.0	1.043	1.0436	1.0434330	0.9583	0.9583	0.958375
7.0		1.1786	1.1783750	0.8485	0.8485	0.848627
10.0	1.344	1.3391	1.3387960	0.7468	0.7468	0.746940

Effects of several values of M on the velocity $f'(\eta)$ profile and the temperature $\theta(\eta)$ profiles for NH, CWT and CHF cases are displayed in Figs 2 and 3 to 5, respectively while the remaining parameters are taken constant. From these figures, it is observed that the velocity within the boundary layer grows-up along to the enhancing nature of M. Subsequently, it is noted that the temperature decreases significantly with the raising values of M in all three considered cases while in the case of NH, the reverse circumstance appear for $\eta > 1.5$. It is also apparent that the actual M impact is negligible in all cases for higher values of η. Physically, the momentum boundary layer thickness reduces over to the booming values of the applied magnetic parameter due to damping effects. This is revealed by the reason that the magnetic field is applied perpendicular to the fluid flow, which has a tendency to generate a drag like force namely Lorentz force which enhances the fluid velocity.

The temperature $\theta(\eta)$ profile for different values of $\Pr$ are given through Fig. 6 to 8 for NH, CWT and CHF cases, respectively, the other parameters are kept

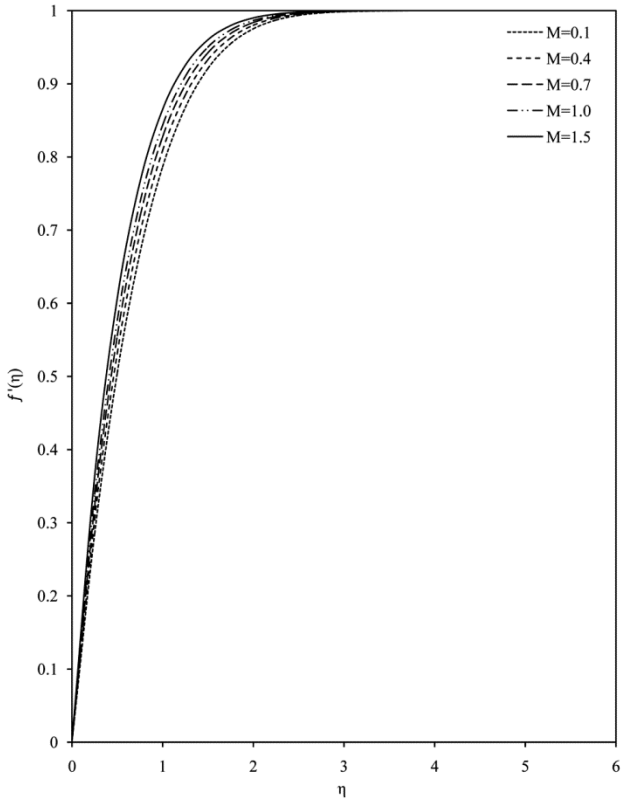

Fig. 2 — Velocity distribution for various values of M.

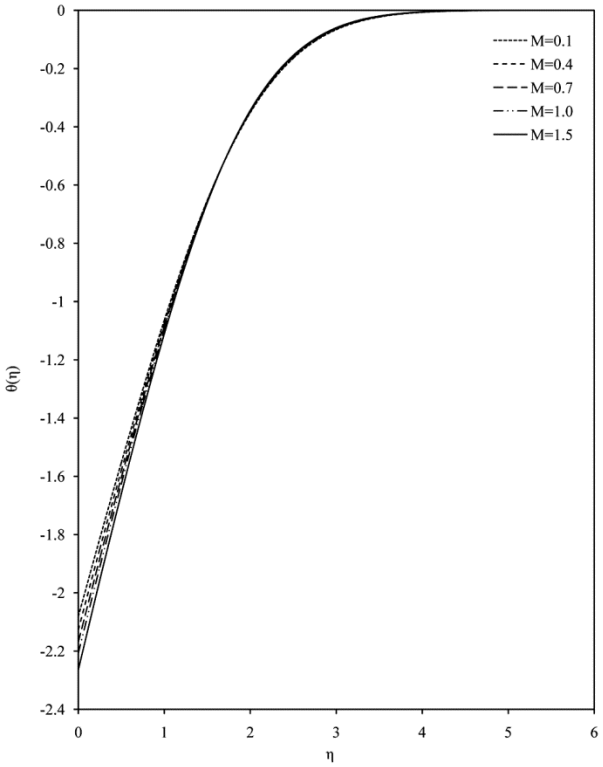

Fig. 3 — Temperature distribution of the NH case for various values of M with $\Pr = 0.7$ and $Ec = 0.1$.

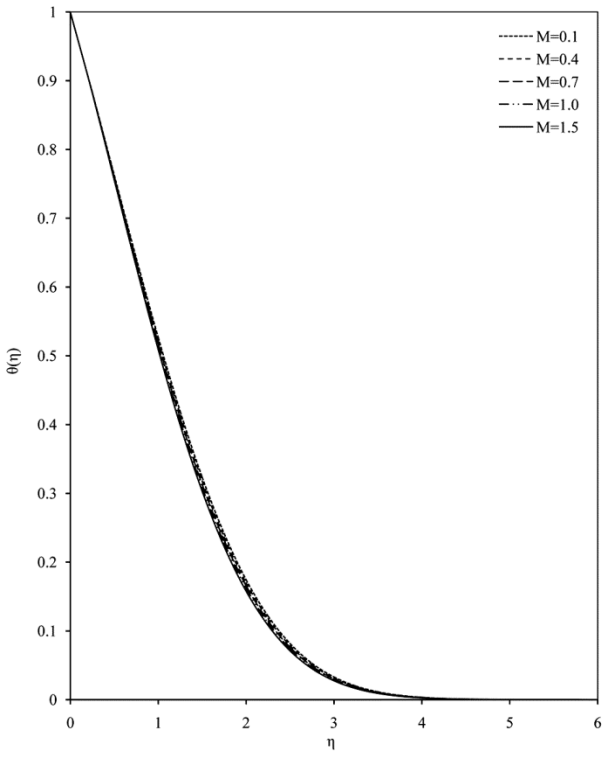

Fig. 4 — Temperature distribution of the CWT case for various values of M with $\Pr = 0.7$ and $Ec = 0.1$.

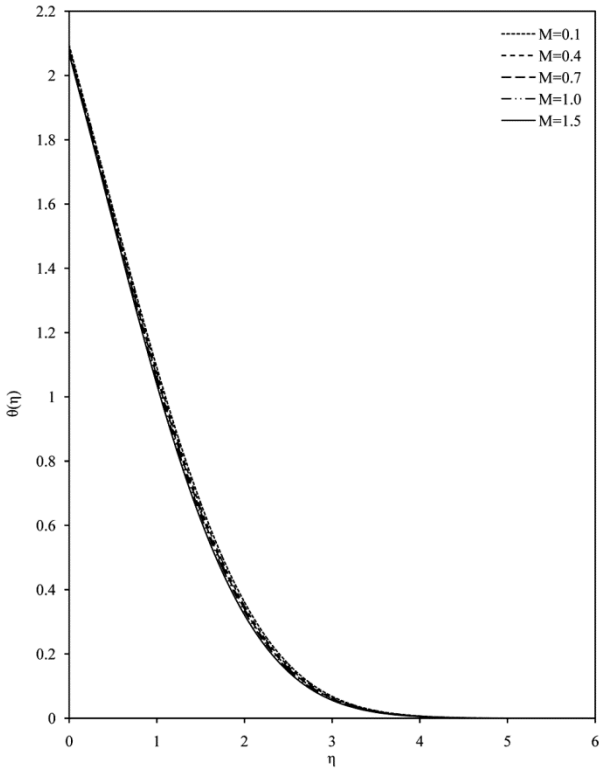

Fig. 5 — Temperature distribution of the CHF case for various values of M with $\Pr = 0.7$ and $Ec = 0.1$.

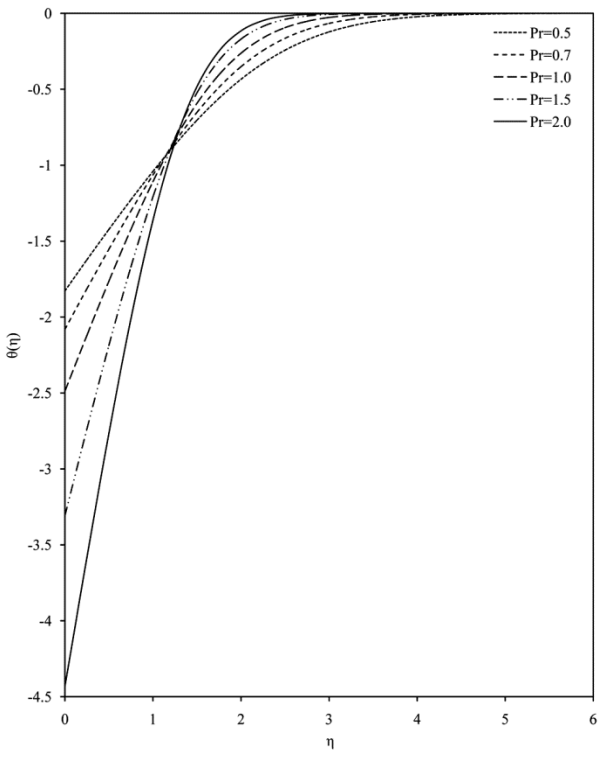

Fig. 6 — Temperature distribution of the NH case for various values of Pr with $M = 0.1$ and $Ec = 0.1$.

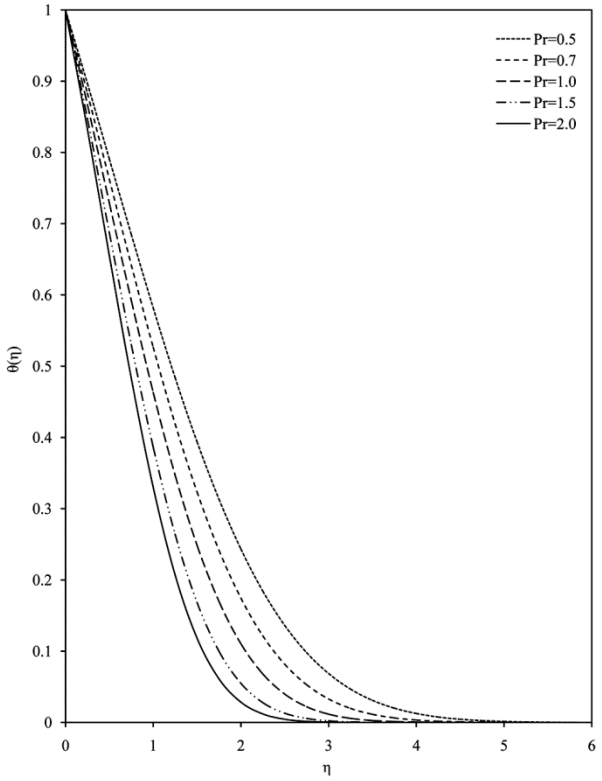

Fig. 7 — Temperature distribution of the CWT case for various values of Pr with $M = 0.1$ and $Ec = 0.1$.

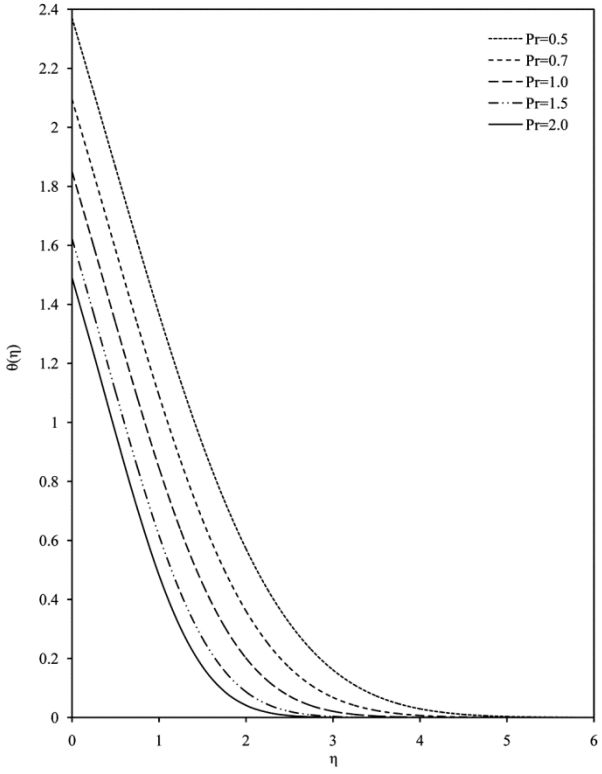

Fig. 8 — Temperature distribution of the CHF case for various values of Pr with $M = 0.1$ and $Ec = 0.1$.

constant. From these figures it is clearly appreciated that the temperature declines over to boosting values of $\Pr$ for all cases but in the case of NH the reverse phenomenon is true for $\eta > 1.25$. This is due to the reason that the fluid temperature asymptotically access to zero in the free stream domain. Therefore, the Prandtl number controls the thermal boundary layers in heat transfer problems, and may be worn to enhance the rate of cooling.

Figures 9 to 11 exhibit the temperature $\theta(\eta)$ distributions in NH, CWT and CHF cases respectively for the development in Ec while the remaining parameters are fixed. It is apparent from these figures, that Ec has the decreasing influence on the dimensionless temperature for the case of NH. Furthermore, the temperature field evolves along with the increasing values of Ec in the CWT and CHF cases respectively. This is because of the greater values of the Eckert number lead a significant generation of heat being viscous dissipation nearby the plate. Thus, viscous dissipation in a flow near the stagnation point is benign to attain the temperature.

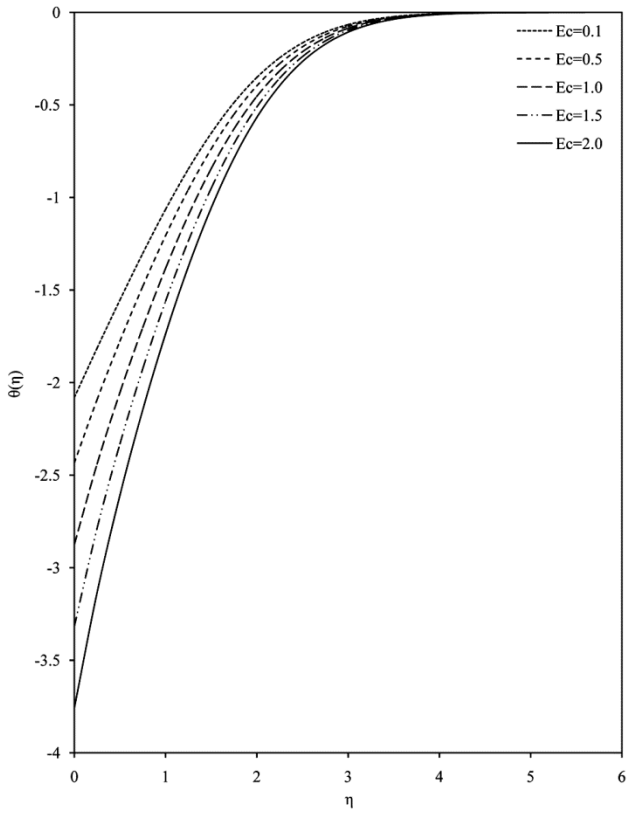

Fig. 9 — Temperature distribution of the NH case for various values of Ec with $M = 0.1$ and $\Pr = 0.7$.

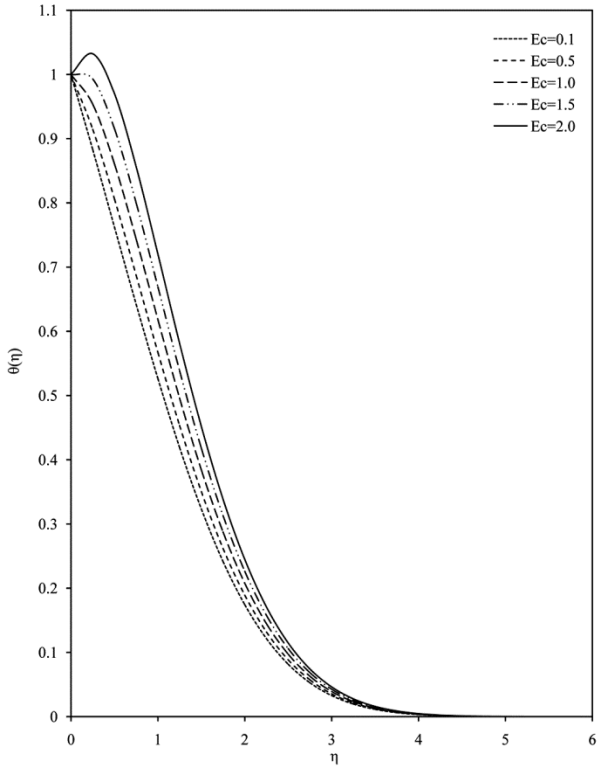

Fig. 10 — Temperature distribution of the CWT case for various values of Ec with $M = 0.1$ and $\Pr = 0.7$.

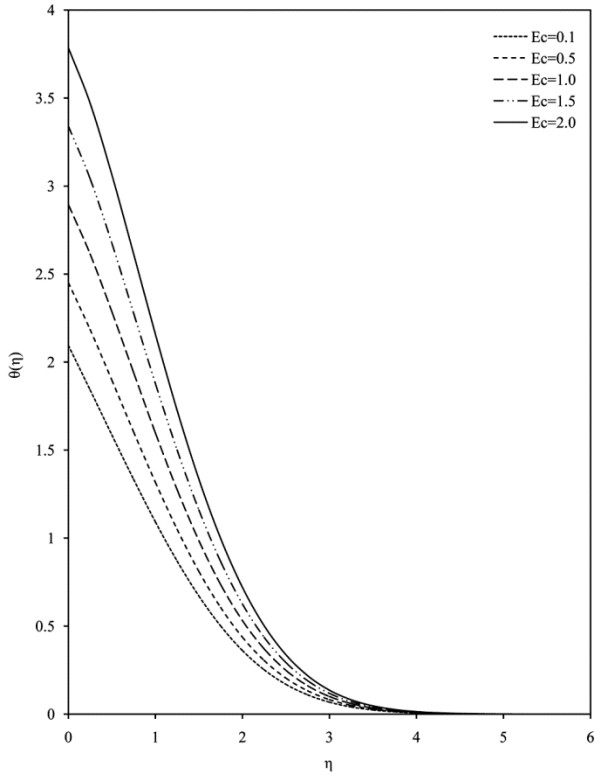

Fig. 11 — Temperature distribution of the CHF case for various values of Ec with $M = 0.1$ and $\Pr = 0.7$.

Table 2 — Values of $f''(0)$, $\theta'(0)$ and $\theta(0)$ for various values of M, Pr and Ec.

M	Pr	Ec	$f''(0)$	$\theta'(0)$ (NH)	$-\theta'(0)$ (CWT)	$\theta(0)$ (CHF)
0.1	0.7	0.1	1.272181	1.08173	0.4539928	2.095671
0.4			1.384316	1.128029	0.451467	2.086313
0.7			1.488169	1.169857	0.4488157	2.079388
1.0			1.585331	1.208139	0.4460865	2.074238
1.5			1.7353606	1.265761	0.4414438	2.068479
0.1	0.5			0.8285029	0.4029627	2.371311
	1.0			1.489497	0.511926	1.850961
	1.5			2.309527	0.5815766	1.623709
	2.0			3.434646	0.632513	1.491046
	0.7	0.5		1.43526	0.276638	2.451568
		1.0		1.877172	0.0549449	2.896439
		1.5		2.3190838	-0.1667483	3.341310
		2.0		2.760995	-0.388442	3.786181

Variation of the surface shear stress $f''(0)$ and the surface heat flux $\theta'(0)$ in the cases of NH and CWT for different value of M, Pr, and Ec are demonstrated in Table 2, taking other parameters constant. Table indicates that the wall shear stress $f''(0)$ increases over to the raising values of M. It is also clear from this table that the values of the surface shear stress are positive for all values of M. Because, positive sign of wall shear stress signifies that fluid utilizes a drag type force on the wall in this case. The heat transfer rate $\theta'(0)$ increases with the enlarging values of M, Pr, and Ec in the cases of NH. Further, the surface heat flux $\theta'(0)$ increases with the step-up in M and Ec even though an opposite behavior is noted for Pr in the case of CWT. Practically, positive sign of the surface heat flux signifies that there is a heat flow to the surface and conversely.

8 Concluding Notes

Impact of Newtonian heating on the magnetohydrodynamic flow nearby the stagnation domain in comparisons of constant wall temperature and constant heat flux presented theoretically. The governing conservation equations were converted into a structure of ordinary differential equations and numerically solved via Galerkin finite element method in association with the Gauss elimination technique. Computational values of the velocity, the temperature, the local skin friction coefficient and the local Nusselt number at the surface were demonstrated along to the magnetic parameter, the Prandtl number and the Eckert number. Main observations of present analysis is remarked as:

(i) The velocity is derived to be increased, allied with a production in the surface velocity gradient, and so the shear stress increased in the presence of the magnetic field. Until, the wall temperature decreases with the applied magnetic parameter in all three cases. It is also noticeable that behavior of the temperature in NH case slightly changes after eta greater than 1.5. Moreover, the surface heat transfer rate has an increasing effect in the cases of NH and CWT as the enlarging value of the magnetic parameter.

(ii) Impact of enhancing nature of the Prandtl number tends to decline the temperature profile for all three considered cases. In addition, for the case of NH, the behavior of the temperature profile becomes quite opposite after the point $\eta \approx 1.25$. Although, the surface heat flux for the case of NH increases with the enlarging value of the Prandtl number but adverse phenomenon is noted in the case of CWT.

(iii) Finally, the temperature profile decreases along with the rising behavior of the Eckert number in the case of NH while a reverse impact is observed in the case of CWT and CHF. Consequently, increasing the Eckert number will produce an increment in the rate of heat transfer for NH and CWT cases.

References

1 Nield D A & Bejan A, *Convection in porous media* (Springer, New York), 2012.

2 Shang D, *Theory of heat transfer with forced convection film flows. Chapter 3* (Heat Mass Transfer, Springer, New York), 2010.

3 Seddeek M A, *J Appl Mech Tech Phys*, 43 (2002) 13.

4 El-Amin M F, *J Magn Magn Mater*, 263 (2003) 337.

5 Duwairi H M, *Int J Numer Methods Heat Fluid Flow*, 15 (2005) 429.
6 Merkin J H & Pop I, *Commun Nonlinear Sci Numer Simul*, 16 (2011) 3602.
7 Sasmal C, Shyam R & Chhabra R P, *Int J Heat Mass Transfer*, 63 (2013) 51.
8 Chaudhary S & Kumar P, *Meccanica*, 49 (2014) 69.
9 Satish N & Venkatasubbaiah K, *Appl Therm Eng*, 100 (2016) 987.
10 Mohseni M M, Tissot G & Badawi M, *Int J Heat Fluid Flow*, 71 (2018) 442.
11 Atashafrooz M, Sheikholeslami M, Sajjadi H & Delouei A A, *J Magn Magn Mater* 478 (2019) 216.
12 Sharma R P & Paul A, *Indian J Pure Appl Phys*, 57 (2019) 205.
13 Hiemenz K, *Dingl Polytech J*, 326 (1911) 321.
14 Homann F, *Z Angew Math Mech*, 16 (1936) 153.
15 Eckert E R G, *VDI Forsch*, 461 (1942).
16 Mahapatra T R & Gupta A S, *Heat Mass Transfer*, 38 (2002) 517.
17 Lok Y Y, Amin N & Pop I, *Acta Mech*, 186 (2006) 99.
18 Jat R N & Chaudhary S, *Z Angew Math Phys*, 61 (2010) 1151.
19 Mahapatra T R & Nandy S K, *Meccanica*, 48 (2013) 23.
20 Chaudhary S & Choudhary M K, *Indian J Pure Appl Phys*, 54 (2016) 209.
21 Mahapatra T R & Sidui S, *Euro J Mech- B/Fluids*, 75 (2019) 199.
22 Dholey S, *Z Angew Math Phys*, 70 (2019) 10.
23 Fang T G & Wang F J, *Appl Math Mech*, 41 (2020) 51.
24 Merkin J H, *Int J Heat Fluid Flow*, 15 (1994) 392.
25 Pop I, Lesnic D & Ingham D B, *Hybrid Meth Eng*, 2 (2000) 31.
26 Lesnic D, Ingham D B & Pop I, *J Porous Media*, 3 (2000) 227.
27 Merkin J H, Nazar R & Pop I, *J Eng Math*, 74 (2012) 53.
28 Hayat T, Ali S, Awais M & Alhuthali M S, *Appl Math Mech-Engl Ed*, 36 (2015) 61.
29 Kushwaha H M & Sahu S K, *J Inst Engin (India): Series C*, 98 (2017) 553.
30 Chaudhary S, Kanika K M & Choudhary M K, *Indian J Pure Appl Phys*, 56 (2018) 931.
31 Aghayari R, Rohani S, Ghasemi N, Heiran E N K & Mazaheri H, *Heat Mass Transfer*, 56 (2020) 1051.
32 Andersson H I, *Acta Mech*, 95 (1992) 227.
33 Mahapatra T R & Gupta A S, *Acta Mech*, 152 (2001) 191.
34 Abel M S & Mahesha N, *Appl Math Model*, 32(2008) 1965.
35 Chaudhary S, Choudhary M K & Sharma R, *Meccanica*, 50 (2015) 1977.
36 Chaudhary S & Choudhary M K, *Eng Comput*, 35 (2018) 1675.
37 Benos L & Sarris I E, *Int J Heat Mass Transfer*, 130 (2019) 862.
38 Chaudhary S & Kanika K M, *J Porous Media*, 23 (2020) 27.
39 Rao P S, Prakash O, Mishra S R & Sharma R P, *Heat Transfer*, 49 (2020) 1842.
40 Salleh M Z, Nazar R & Pop I, *Chem Eng Commun*, 196 (2009) 987.
41 Bansal J L, *Magnetofluiddynamics of viscous fluids* (Jaipur Pub House, India), 1994.